

# Frequency comb generation by CW laser injection into a quantum-dot mode-locked laser

T. J. Pinkert,<sup>1</sup> E. J. Salumbides,<sup>1</sup> M. S. Tahvili,<sup>2</sup> W. Ubachs,<sup>1</sup>  
E. A. J. M. Bente,<sup>2</sup> and K. S. E. Eikema<sup>1,\*</sup>

<sup>1</sup>*LaserLaB, Department of Physics and Astronomy, VU University,  
De Boelelaan 1081, 1081 HV Amsterdam, The Netherlands*

<sup>2</sup>*COBRA Research Institute, Technische Universiteit Eindhoven,  
Den Dolech 2, 5600 MB Eindhoven, The Netherlands*

[\\*k.s.e.eikema@vu.nl](mailto:k.s.e.eikema@vu.nl)

**Abstract:** We report on frequency comb generation at 1.5  $\mu\text{m}$  by injection of a CW laser in a hybridly mode-locked InAs/InP two-section quantum-dot laser (HMLQDL). The generated comb has  $> 60$  modes spaced by  $\sim 4.5$  GHz and a  $-20$  dBc width of  $> 100$  GHz (23 modes) at  $> 30$  dB signal to background ratio. Comb generation was observed with the CW laser (red) detuned more than 20 nm outside the HMLQDL spectrum, spanning a large part of the gain spectrum of the quantum dot material. It is shown that the generated comb is fully coherent with the injected CW laser and RF frequency used to drive the hybrid mode-locking. This method of comb generation is of interest for the creation of small and robust frequency combs for use in optical frequency metrology, high-frequency ( $> 100$  GHz) RF generation and telecommunication applications.

© 2012 Optical Society of America

**OCIS codes:** (130.3120) Integrated optics devices; (130.4110) Modulators; (230.2090) Electro-optical devices; (250.5960) Semiconductor lasers.

---

## References and links

1. R. Holzwarth, T. Udem, T. W. Hänsch, J. C. Knight, W. J. Wadsworth, and P. S. J. Russell, "Optical frequency synthesizer for precision spectroscopy," *Phys. Rev. Lett.* **85**, 2264–2267 (2000).
2. D. Jones, S. Diddams, J. Ranka, A. Stentz, R. Windeler, J. Hall, and S. Cundiff, "Carrier-envelope phase control of femtosecond mode-locked lasers and direct optical frequency synthesis," *Science* **288**, 635–639 (2000).
3. H. S. Margolis, G. P. Barwood, G. Huang, H. A. Klein, S. N. Lea, K. Szymaniec, and P. Gill, "Hertz level measurement of the optical clock frequency in a single  $^{88}\text{Sr}^+$  ion," *Science* **306**, 1355–1358 (2004).
4. P. Balling, P. Křen, P. Mašika, and S. A. van den Berg, "Femtosecond frequency comb based distance measurement in air," *Opt. Express* **17**, 9300–9313 (2009).
5. T. Steinmetz, T. Wilken, C. Araujo-Hauck, R. Holzwarth, T. W. Hänsch, L. Pasquini, A. Manescau, S. D'Odorico, M. T. Murphy, T. Kentischer, W. Schmidt, and T. Udem, "Laser frequency combs for astronomical observations," *Science* **321**, 1335–1337 (2008).
6. S. A. Diddams, L. Hollberg, and V. Mbele, "Molecular fingerprinting with the resolved modes of a femtosecond laser frequency comb," *Nature (London)* **445**, 627–630 (2007).
7. S. Anantathanasarn, R. Nötzel, P. J. van Veldhoven, F. W. M. van Otten, Y. Barbarin, G. Servanton, T. de Vries, E. Smalbrugge, E. J. Geluk, T. J. Eijkemans, E. A. J. M. Bente, Y. S. Oei, M. K. Smit, and J. H. Wolter, "Wavelength controlled InAs/InP quantum dots for telecom laser applications," *Microelectron. J.* **37**, 1461–1467 (2006).
8. Z. G. Lu, J. R. Liu, S. Raymond, P. J. Poole, P. J. Barrios, and D. Poitras, "312-fs pulse generation from a passive C-band InAs/InP quantum dot mode-locked laser," *Opt. Express* **16**, 10835–10840 (2008).

9. R. Rosales, K. Merghem, A. Martinez, A. Akrou, J.-P. Turrenc, A. Accard, F. Lelarge, and A. Ramdane, "InAs/InP quantum-dot passively mode-locked lasers for 1.55- $\mu\text{m}$  applications," *IEEE J. Sel. Top. Quantum Electron.* **17**, 1292–1301 (2011).
10. E. U. Rafailov, M. A. Cataluna, W. Sibbett, N. D. Il'inskaya, Y. M. Zadiranov, A. E. Zhukov, V. M. Ustinov, D. A. Livshits, A. R. Kovsh, and N. N. Ledentov, "High-power picosecond and femtosecond pulse generation from a two-section mode-locked quantum-dot laser," *Appl. Phys. Lett.* **87**, 081107 (2005).
11. E. U. Rafailov, M. A. Cataluna, and W. Sibbett, "Mode-locked quantum-dot lasers," *Nature Photonics* **1**, 395–401 (2007).
12. K. W. Holman, D. J. Jones, J. Ye, and E. P. Ippen, "Orthogonal control of the frequency comb dynamics of a mode-locked laser diode," *Opt. Lett.* **28**, 2405–2407 (2003).
13. S. A. Diddams, M. Kirchner, T. Fortier, D. Braje, A. M. Weiner, and L. Hollberg, "Improved signal-to-noise ratio of 10 GHz microwave signals generated with a mode-filtered femtosecond laser frequency comb," *Opt. Express* **17**, 3331–3340 (2009).
14. T. Habruseva, S. O'Donoghue, N. Rebrova, D. A. Reid, L. P. Barry, S. P. Hegarty, D. Rachinskii, and G. Huyet, "Quantum-dot mode-locked lasers with dual mode optical injection," *IEEE Photonics Tech. Lett.* **22**, 359–361 (2010).
15. N. K. Fontaine, R. P. Scott, J. Cao, A. Karalar, W. Jiang, K. Okamoto, J. P. Heritage, B. H. Kolner, and S. J. B. Yoo, "32 phase  $\times$  32 amplitude optical arbitrary waveform generation," *Opt. Lett.* **32**, 865–867 (2007).
16. H. Schmeckebier, G. Fiol, C. Meuer, D. Arsenijević, and D. Bimberg, "Complete pulse characterization of quantum-dot mode-locked lasers suitable for optical communication up to 160 Gbit/s," *Opt. Express* **18**, 3415–3425 (2010).
17. S. Arahira, H. Takahashi, K. Nakamura, H. Yaegashi, and Y. Ogawa, "Polarization-, wavelength-, and filter-free all-optical clock recovery in a passively mode-locked laser diode with orthogonally pumped polarization-diversity configuration," *IEEE J. Quantum Electron.* **45**, 476–487 (2009).
18. H. Takara, T. Ohara, K. Mori, K. Sato, E. Yamada, Y. Inoue, T. Shibata, M. Abe, T. Morioka, and K.-I. Sato, "More than 1000 channel optical frequency chain generation from single supercontinuum source with 12.5 GHz channel spacing," *Electron. Lett.* **36**, 2089–2090 (2000).
19. T. Kuri, T. Nakasyotani, H. Toda, and K.-I. Kitayama, "Characterizations of supercontinuum light source for WDM millimeter-wave-band radio-on-fiber systems," *IEEE Photonics Tech. Lett.* **17**, 1274–1276 (2005).
20. T. Kuri, H. Toda, J. Olmos, and K. Kitayama, "Reconfigurable dense wavelength-division-multiplexing millimeter-waveband radio-over-fiber access system technologies," *J. Lightwave Tech.* **28**, 2247–2257 (2010).
21. R. Zhou, S. Latkowski, J. O'Carroll, R. Phelan, L. P. Barry, and P. Anandarajah, "40nm wavelength tunable gain-switched optical comb source," *Opt. Express* **19**, B415–B420 (2011).
22. W. Shieh, H. Bao, and Y. Tang, "Coherent optical OFDM: theory and design," *Opt. Express* **16**, 841–859 (2008).
23. M. J. R. Heck, E. J. Salumbides, A. Renault, E. A. J. M. Bente, Y.-S. Oei, M. K. Smit, R. van Veldhoven, R. Nötzel, K. S. E. Eikema, and W. Ubachs, "Analysis of hybrid mode-locking of two-section quantum dot lasers operating at 1.5  $\mu\text{m}$ ," *Opt. Express* **17**, 18063–18075 (2009).
24. M. J. R. Heck, A. Renault, E. A. J. M. Bente, Y.-S. Oei, M. K. Smit, K. S. E. Eikema, W. Ubachs, S. Anantathanasarn, and R. Nötzel, "Passively mode-locked 4.6 and 10.5 GHz quantum dot laser diodes around 1.55  $\mu\text{m}$  with large operating regime," *IEEE J. Sel. Top. Quantum Electron.* **15**, 634–643 (2009).
25. M. J. R. Heck, E. A. J. M. Bente, B. Smalbrugge, Y.-S. Oei, M. K. Smit, S. Anantathanasarn, and R. Nötzel, "Observation of Q-switching and mode-locking in two-section InAs/InP (100) quantum dot lasers around 1.55  $\mu\text{m}$ ," *Opt. Express* **15**, 16292–16301 (2007).
26. S. Anantathanasarn, R. Nötzel, P. J. van Veldhoven, F. W. M. van Otten, Y. Barbarin, G. Servanton, T. de Vries, E. Smalbrugge, E. J. Geluk, T. J. Eijkemans, E. A. J. M. Bente, Y.-S. Oei, M. K. Smit, and J. H. Wolter, "Lasing of wavelength-tunable (1.55  $\mu\text{m}$  region) InAs/InGaAsP/InP (100) quantum dots grown by metal organic vapor-phase epitaxy," *Appl. Phys. Lett.* **89**, 073115 (2006).
27. M. S. Tahvili, L. Du, M. J. R. Heck, R. Nötzel, M. K. Smit, and E. A. J. M. Bente, "Dual-wavelength passive and hybrid mode-locking of 3, 4.5 and 10 GHz InAs/InP(100) quantum dot lasers," *Opt. Express* **20**, 8117–8135 (2012).
28. G. P. Agrawal and N. A. Olsson, "Self-phase modulation and spectral broadening of optical pulses in semiconductor laser amplifiers," *IEEE J. Quantum Electron.* **25**, 2297–2306 (1989).
29. P. Balling, M. Fischer, P. Kubina, and R. Holzwarth, "Absolute frequency measurement of wavelength standard at 1542nm: acetylene stabilized DFB laser," *Opt. Express* **13**, 9169–9201 (2005).
30. R. Prasanth, J. E. M. Haverkort, A. Deepthy, E. W. Bogaart, J. J. G. M. van der Tol, E. A. Patent, G. Zhao, Q. Gong, P. J. van Veldhoven, R. Nötzel, and J. H. Wolter, "All-optical switching due to state filling in quantum dots," *Appl. Phys. Lett.* **84**, 4059–4061 (2004).
31. T. Healy, F. C. Garcia Gunning, and A. D. Ellis, "Multi-wavelength source using low drive-voltage amplitude modulators for optical communications," *Opt. Express* **15**, 2981–2986 (2007).

## 1. Introduction

Frequency comb lasers [1,2] have been around since the early 2000's, enabling highly-accurate optical time and frequency measurements resulting in many applications [3–6]. Integrated optical frequency comb lasers would pave the way to an even broader application of comb technology because of low fabrication and maintenance costs. Mode-locked quantum dot lasers (MLQDL) are interesting for this application as they have a broad gain bandwidth ( $> 100$  nm) required for short pulse generation [7–11]. Further on-chip integration with an optical amplifier, highly non-linear media for spectral broadening and an  $f-2f$  interferometer (for carrier envelope offset frequency ( $f_{\text{CEO}}$ ) detection), and feedback electronics for orthogonal control of  $f_{\text{rep}}$  and  $f_{\text{CEO}}$  [12], could lead to fully integrated, self-referenced frequency comb laser designs.

Because of their small size, these lasers have pulse repetition rates ( $f_{\text{rep}}$ ) in the range of a GHz up to hundreds of GHz, which is a useful property for e.g. low-noise microwave generation [13, 14], accurate calibration of spectrometers [5], and optical arbitrary waveform generation [15]. Apart from metrology applications, high repetition rate frequency combs are of interest for telecommunication applications as highly stable pulse train emitters for applications such as optical time-domain multiplexing (OTDM) [16] or all-optical clock recovery [17]. With their wide optical spectrum and stabilized mode spacing, ultra-high repetition rate frequency combs are attractive for application in wavelength-division multiplexed (WDM) systems and also as multi-wavelength light sources [18–21]. The coherence of frequency comb modes can be exploited in Coherent Optical Orthogonal Frequency Division Multiplexing (CO-OFDM) [22].

In this work we report on the generation of optical side bands (modes in the form of a frequency comb) on a CW diode laser injected into two-section InAs/InP (H)MLQDL devices [23, 24] working at  $1.5 \mu\text{m}$ . This frequency comb generation appears to be independent of the laser action and shows that the device works as an electro-optical modulator, producing equally spaced and coherent modes. The generated comb has been characterized using two narrow linewidth CW lasers and an  $\text{Er}^{3+}$ -fiber based frequency comb laser.

## 2. Description of the HMLQDL and the experimental setup for optical injection

The (H)MLQDL's used in this experiment are 9 mm long ( $f_{\text{rep}} \sim 4.5$  GHz), two-section InAs/InP (100) Fabry-Pérot type ridge-waveguide devices, produced by metal-organic vapor-phase epitaxy [23–26]. The  $2 \mu\text{m}$  wide wave guides have been produced using reactive ion etching and the mirrors are formed by the cleaved facets ( $\sim 31\%$  reflectivity). The saturable absorber section had a length of  $360 \mu\text{m}$  (4%).

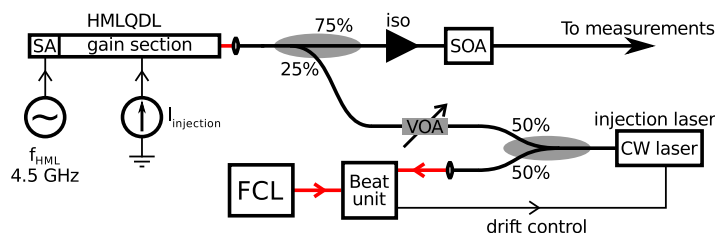


Fig. 1. Setup for studies of CW injected QDL device behavior. HMLQDL: hybridly mode-locked quantum dot laser, iso: isolator, SOA: semiconductor optical amplifier, FCL: frequency comb laser, VOA: variable optical attenuator, thin black lines: electrical signals, red lines: free space optical path, thick black lines: fiber optics.

Figure 1 shows part of the setup used to investigate the behavior of the HMLQDL device when a CW laser is injected. The effects of hybrid mode-locking were reported previously [23]. The HMLQDL is mounted on a copper plate that is temperature stabilized to  $10^\circ\text{C}$  to optimize

the gain. To prevent condensation, the setup is flushed with nitrogen gas. An Agilent N5181A RF generator with a frequency doubling setup and an amplifier (maximum output 25 dBm) was used to generate the hybrid mode-locking voltage (typically 6–11 V<sub>pp</sub>) that was applied to the SA section of the chip via a bias tee (no bias voltage applied) and a three point ground-signal-ground probe (coupling efficiency to SA section unknown).

The output of the laser was coupled into an anti-reflection coated lensed fiber using a piezo controlled three axis translation stage (estimated coupling loss 3–5 dB). Light of a CW laser (Toptica DL 100/pro, linewidth 100 kHz, power ~ 40 mW, internal isolator) was adjusted in power with a variable attenuator (0–6.2 mW) and injected into the HMLQDL device via the 25% port of a fused fiber splitter/combiner. The standard single-mode fiber was manipulated to optimize the polarization of the injected light. The injection laser was optically locked to one of the modes of a Menlo Systems FC1500 Er<sup>3+</sup>-doped fiber frequency comb laser (FCL) to precisely control the optical injection frequency ( $f_{\text{injection}}$ ). The HMLQDL output (75% port) was sent through an optical isolator and amplified in a semiconductor optical amplifier (SOA, type JDS CQF 872/108C) to about 40mW in order to have sufficient optical power for further analysis. It has been checked that the SOA did not induce additional non-linear effects.

### 3. CW injection of the HMLQDL

As frequency comb applications benefit from narrow modes, injection locking of the (H)MLQDL to reduce the linewidth of the (H)MLQDL modes was attempted. No injection locking and related narrowing of the HMLQDL modes has been observed, presumably due to the low resonator Q (and resulting mode widths of > 100 MHz) of the devices which makes it hard to influence these modes by narrow CW laser injection. However, narrow linewidth peaks were observed in the heterodyne spectrum which were independent of the HMLQDL's native mode structure but exhibited a spacing of  $f_{\text{HML}}$ .

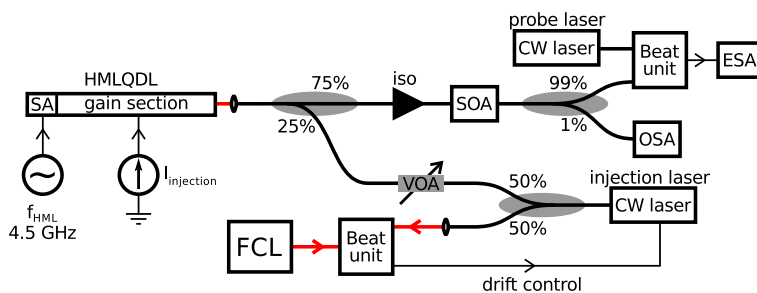


Fig. 2. Setup used to characterize the mode structure of the QDL with CW laser injection. HMLQDL: hybridly mode-locked quantum dot laser, iso: isolator SOA: semiconductor optical amplifier, ESA: electrical spectrum analyzer, OSA: optical spectrum analyzer, FCL: frequency comb laser, VOA: variable optical attenuator, thin black lines: electrical signals, red lines: free space optical path, thick black lines: fiber optics.

The setup of Fig. 2 was used where the probe laser is a Toptica DL 100/pro CW laser (tunable 1490–1590 nm). This probe laser was used to make a heterodyne beat with the output of the CW injected QDL. The CW injection laser was placed at an arbitrary wavelength of ~ 1515 nm where native QDL modes are visible in the heterodyne spectrum. The probe laser was blue detuned with respect to the injection laser with ~ 7.9 GHz. The spectrum of this heterodyne beat was recorded with an Agilent 4440A electrical spectrum analyzer (ESA), showing the (optical) sum and difference frequencies between the QDL laser output and the probe laser in the frequency range recorded.

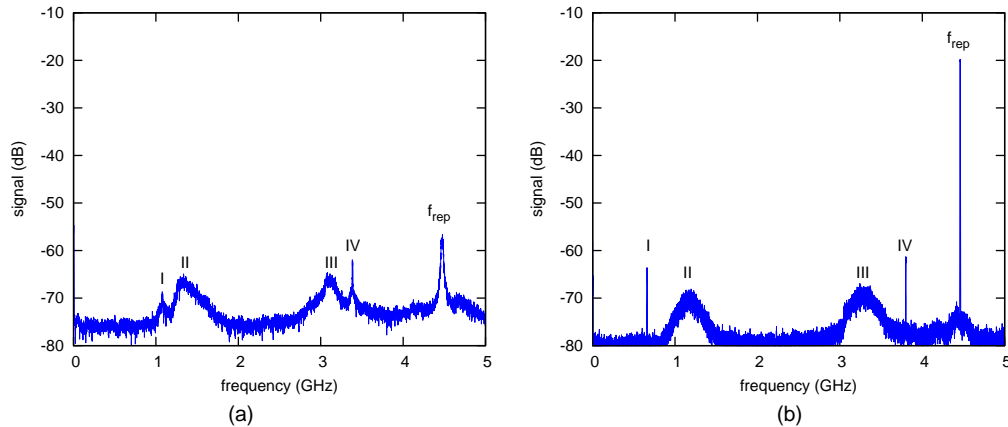


Fig. 3. Optical heterodyne beat signals of the QDL light including the modulated CW injection laser with the probe laser measured with the electrical spectrum analyzer (ESA). The wavelength of the injection laser was tuned inside the (H)MLQDL's spectrum at  $\sim 1515$  nm. QDL modes are visible as broad peaks (II and III) at  $I_{\text{injection}} \sim 645$  mA. (a) Passively mode-locked QDL.  $f_{\text{rep}} \sim 4.5$  GHz, modes 1 (IV) and 2 (I) of the modulated CW injection laser are visible at  $\sim 3.4$  and  $\sim 1.1$  GHz. (b) Hybridly mode-locked QDL.  $f_{\text{rep}} = 4.46$  GHz, modes of the modulated CW injection laser are visible at  $\sim 3.8$  (IV) and  $\sim 0.7$  GHz (I).

Figure 3(a) shows the RF spectrum of the beat of the injected passively mode-locked laser with the probe laser. The direct beat between the injection and probe lasers (located at  $\sim 7.9$  GHz) is not visible in the recorded spectrum. The first two modulation side bands are visible at  $\sim 3.4$  (IV) and  $\sim 1.1$  GHz (I, negative beat sign) as narrow spikes, while native modes of the QDL (II and III) are visible as broad peaks around  $\sim 1.5$  and  $\sim 3$  GHz. The narrow spikes (I and IV) disappear when no CW laser light is injected, while the QDL modes stay the same. When the frequency of the injected laser is shifted, the narrow peaks shift the same amount in frequency. The frequency difference between the two narrow peaks is exactly the passive mode-locking frequency of the QDL. The appearance of narrow peaks, the spacing of these peaks and the shifting of the peaks together with (optical) frequency shifts of the injection laser are all clear signs of optical side-band generation on the injected CW laser.

A similar spectrum of the hybridly mode-locked QDL is shown in Fig. 3(b). Again the broad peaks ( $\sim 1.2$  (II) and  $\sim 3.2$  GHz (III)) are native QDL modes, while the narrow spikes at  $\sim 3.8$  (IV) and  $\sim 0.7$  GHz (I) are side bands of the modulated CW injection laser. The repetition rate ( $f_{\text{rep}}$ ) is now fixed by the RF generator at 4.46 GHz.

A number of experiments was performed to further study the modulation imposed on the injected CW laser. It was noted that the modulation was present when the injected CW laser was tuned outside the QDL's spectrum as well, this effect was exploited to study the the modulation with no interference of the native QDL spectrum.

### 3.1. Characterization of the passively mode-locked QDL with an injected CW laser

The setup shown in Fig. 4 has been used to characterize the passively mode-locked QDL by recording the RF and optical spectra without (Fig. 5(a)) and with (Fig. 5(b)) the CW injection laser. About 1% of the SOA output was directed to an ANDO 6315A optical spectrum analyzer (OSA, resolution 0.05 nm), while the remaining 99% was split in two (this splitter is not drawn) and the light of one of the outputs was coupled into an EOT ET-3500 InGaAs photo diode (3

dB bandwidth > 10 GHz) to obtain RF spectra with the ESA. The injection current  $I_{\text{injection}}$  has been varied from 200 mA to 1000 mA in steps of 5 mA. For each value of  $I_{\text{injection}}$  an RF repetition rate spectrum and an optical spectrum of the laser were recorded. This setup has also been used to investigate the influence of the hybrid mode-locking frequency ( $f_{\text{HML}}$ ).

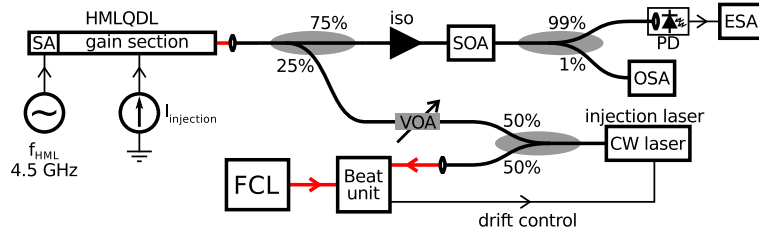


Fig. 4. Setup used to investigate variation of  $I_{\text{injection}}$  and  $f_{\text{HML}}$ . HMLQDL: hybridly mode-locked quantum dot laser, iso: isolator, SOA: semiconductor optical amplifier, PD: photo diode, ESA: electrical spectrum analyzer, OSA: optical spectrum analyzer, FCL: frequency comb laser, VOA: variable optical attenuator, thin black lines: electrical signals, red lines: free space optical path, thick black lines: fiber optics.

The results for the passively mode-locked QDL are shown in Fig. 5. For  $I_{\text{injection}}$  from  $\sim 540$  mA to  $\sim 760$  mA a relatively well defined passive mode-locking repetition rate frequency of  $\sim 4.45$  GHz is seen. In Fig. 5(b) broadening of the CW laser spectrum is visible for  $I_{\text{injection}} > 800$  mA. At  $I_{\text{injection}}$  higher than  $\sim 840$  mA there is no well defined peak found in the RF spectrum, the peaks at various low frequencies up to 2 GHz indicate Q-switching of the laser in this regime. The modulation (with varying current) of the spectral width (clearly seen between 0.5 and 0.8 A) in the optical spectrum and background noise in the RF spectrum, are attributed to the resonance condition of the CW laser in the QDL cavity. The index of refraction of the waveguide varies with the current density and temperature variations caused by changing the current density via  $I_{\text{injection}}$ . The spectral broadening of the injected CW laser, is attributed to a periodic modulation of the losses and refractive index of the SA section due to a fluctuating photo-current caused by the light pulses of the QDL traveling back and forth in the waveguide.

### 3.2. Characterization of the hybridly mode-locked QDL with an injected CW laser

The injection of the QDL was repeated while hybridly mode-locking the QDL laser. The hybrid mode-locking (HML) frequency  $f_{\text{HML}}$  has been chosen for optimal HML at  $I_{\text{injection}} \sim 700$  mA. It's frequency lies in the vicinity of the passive mode-locking frequency (4.45 GHz). The injection current  $I_{\text{injection}}$  has been varied from 200 mA to 1000 mA in steps of 5 mA, and for each value of the current an RF repetition rate and optical spectrum of the laser were recorded. In Fig. 6 and Fig. 7 the RF peak has been artificially broadened in frequency from the kHz resolution band width of the ESA to 10 MHz in order to make this peak visible in the RF spectra.

For below lasing threshold values of  $I_{\text{injection}}$  up to  $\sim 440$  mA the applied RF voltage to the SA section already causes modulation of the injected CW laser, which is visible as an enhanced RF peak in Fig. 6(b) in the RF spectrum. This is an indication that the SA section of the laser works as an electro-optical modulator (EOM) for amplitude and phase. In this case a signal to background ratio of  $> 20$  dB has been measured at  $7f_{\text{HML}}$  mode spacings from the injected CW laser.

At  $I_{\text{injection}}$  above  $\sim 440$  mA the laser is properly hybridly mode-locked (spurious frequencies are more than 50 dB below the HML signal). Spectral broadening of the injected laser has been observed over the entire HMLQDL spectrum and up to  $\sim 25$  nm red detuned from the edge of

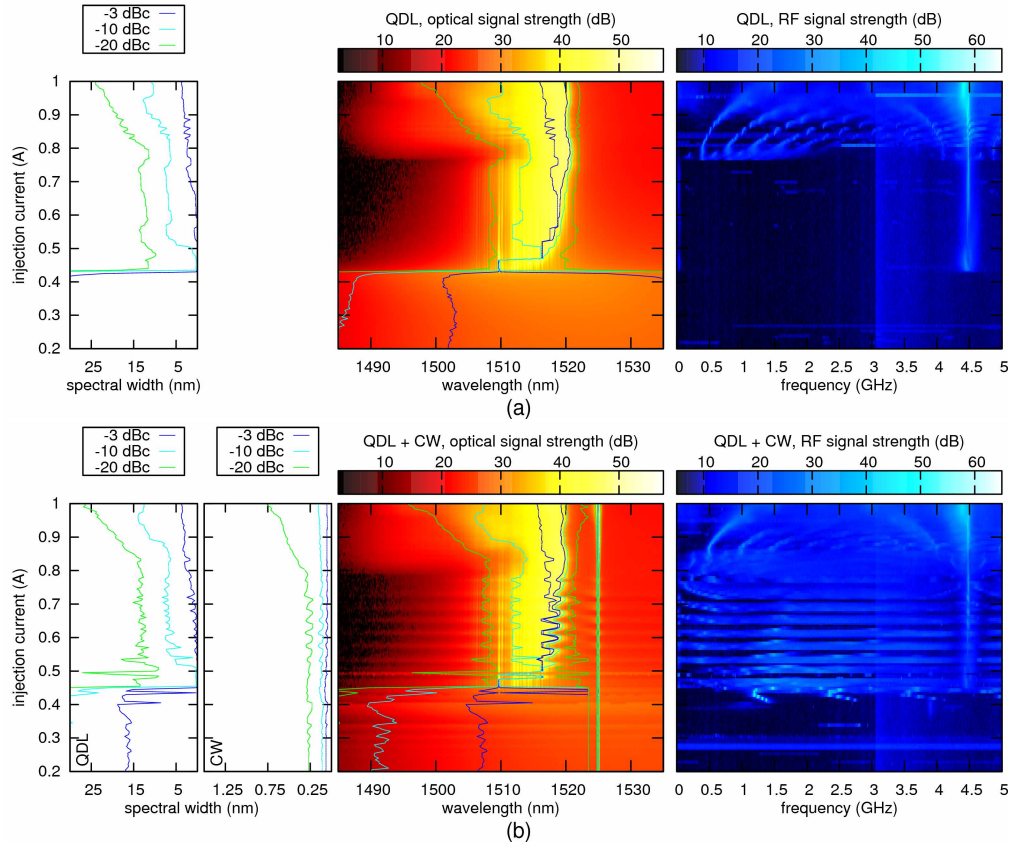


Fig. 5. (a) Spectra of the passively mode-locked QDL. (b) Spectra of the passively mode-locked QDL with injected CW laser at  $\sim 1525$  nm. (left panel) Optical spectral widths of the QDL and the modulated CW injection laser at -3,-10 and -20 dB relative to the peak height. Optical (middle panel) and RF repetition rate (right panel) spectra of the passively mode-locked QDL. The injected optical power was 2.8 mW into the 25% port (Fig 4). The slight background step in the RF spectrum starting at  $\sim 3$  GHz and fading out to  $\sim 4$  GHz is an analyzer artefact.

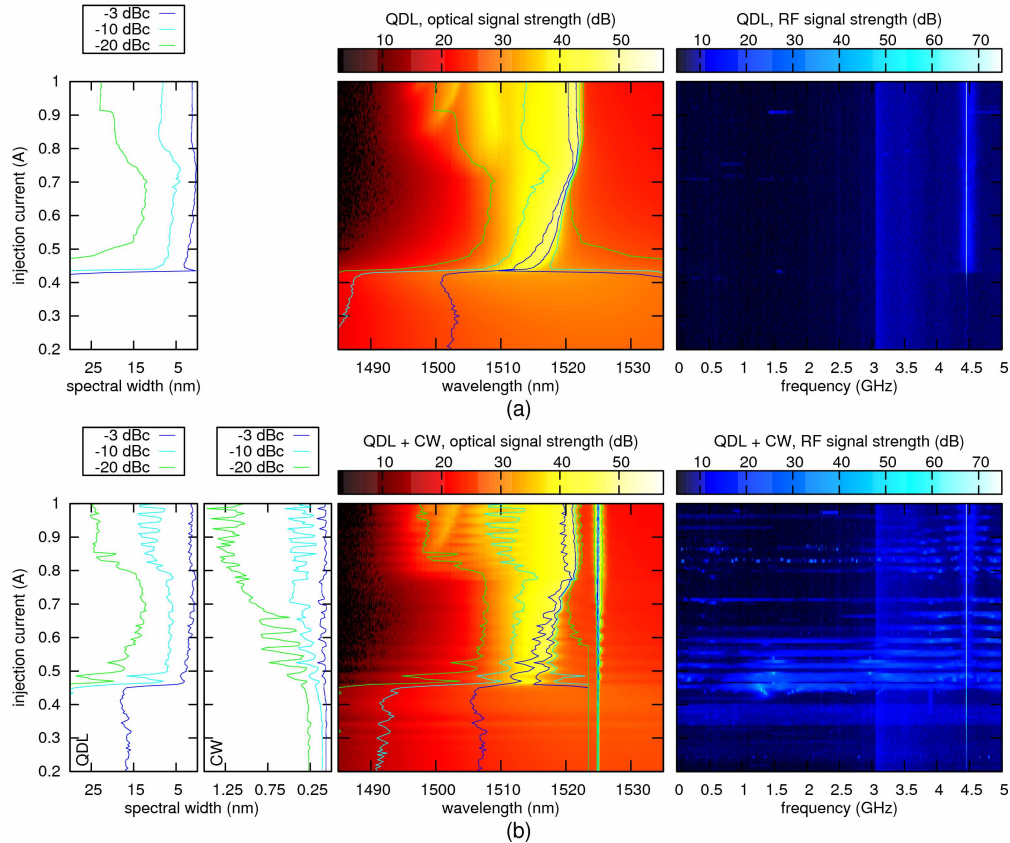


Fig. 6. (a) Spectra of the hybridly mode-locked QDL. (b) Spectra of the hybridly mode-locked QDL with modulated CW injection laser at  $\sim 1525$  nm. (left panel) Optical spectral widths of the QDL and the injected CW laser at -3, -10 and -20 dB relative to the peak height. Optical (middle panel) and RF repetition rate (right panel) spectra of the hybridly mode-locked QDL. The injected optical power was 2.8 mW into the 25% port (Fig 4).

the HMLQDL spectrum. The width of the modulation decreased when increasing the separation between the CW injection wavelength and the edge of the HMLQDL's spectrum. Both Fig. 5 and Fig. 6 show an increased modulation width with increasing  $I_{\text{injection}}$ . Hybrid mode-locking was found to increase the width of the modulation with regard to the passively mode-locked case.

### 3.3. Spectral width of the injected CW laser with varying $I_{\text{injection}}$ and $f_{\text{HML}}$

Since the laser itself undergoes only minor changes in its spectrum while varying the HMLQDL parameters, we will focus on the properties of the modulation imposed by the HMLQDL on the CW laser in the remainder of the article.

In the previous section the influence of  $I_{\text{injection}}$  on the width of the modulation was studied while  $f_{\text{HML}}$  was given a fixed value. To observe the influence of  $f_{\text{HML}}$  on the modulation of the CW laser, it has been varied from 3.9 to 4.9 GHz with a step size of 2 MHz for a fixed value of  $I_{\text{injection}}$  while recording the optical and RF repetition rate spectra. The results are shown in Fig. 7 for  $I_{\text{injection}} = 500$  mA and  $I_{\text{injection}} = 1000$  mA.

Varying  $f_{\text{HML}}$  at a low injection current of 500 mA shows various frequency ranges where



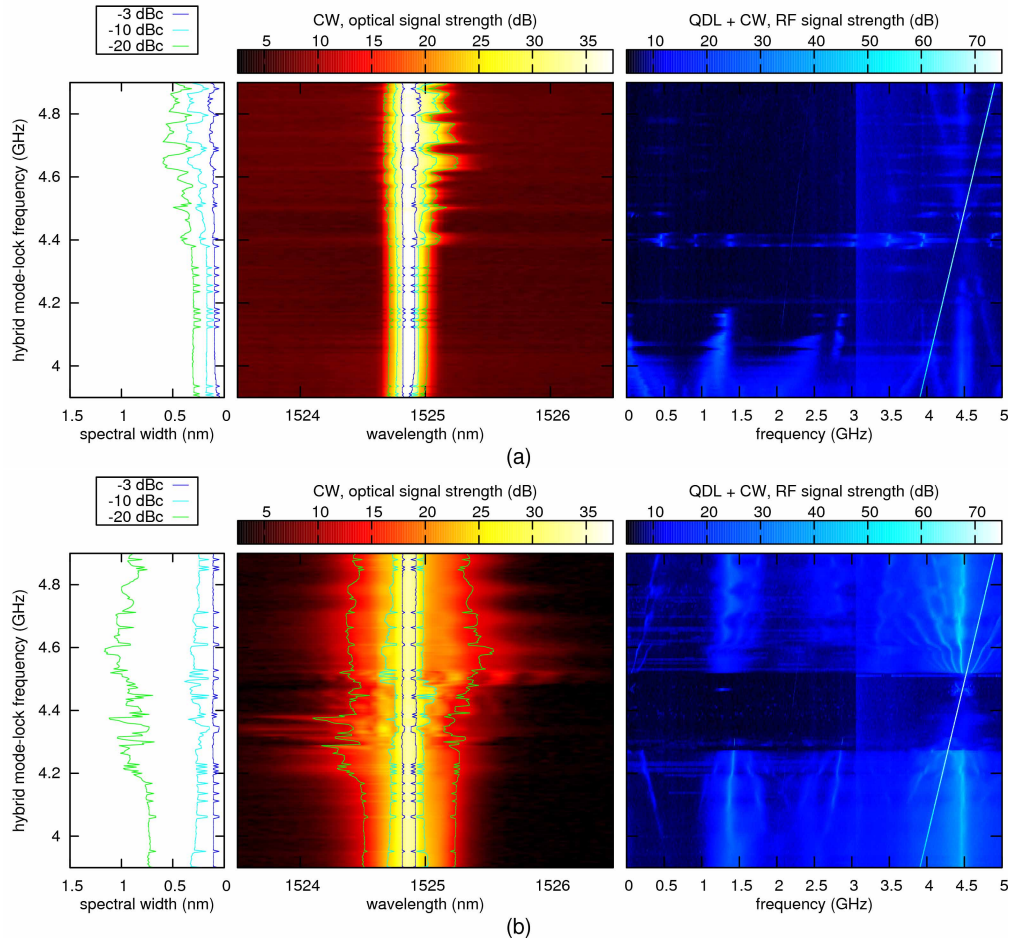


Fig. 7. Spectral width of the modulated CW injection laser as a function of  $f_{HML}$ . Part (a) is for  $I_{injection} = 500$  mA, while part (b) shows the same for  $I_{injection} = 1000$  mA. (left panel) -3, -10 and -20 dB width of the modulated CW injection laser with respect to peak height. (middle panel) Optical spectrum of the modulated CW injection laser only. (right panel) RF repetition rate spectrum of the HMLQDL including the modulated CW injection laser. The injected optical power was 2.8 mW into the 25% port.

the modulation depth is enhanced, mainly for frequencies above the passive mode-locking frequency. Note that the mode-locking frequency of the HMLQDL seems to follow  $f_{\text{HML}}$  over the full frequency range. This is however probably not the case, since the HMLQDL output and the modulated CW light on the detector both cause an RF peak, which masks the proper HML range of the QDL. A slightly enhanced background at the native repetition rate of the QDL up to  $\sim 4.3$  GHz and from  $\sim 4.5$  GHz are an indication that the QDL does not HML properly over the full frequency range, which is consistent with previous results for these lasers [23].

At a high injection current of 1000 mA the modulation depth is larger over the full  $f_{\text{HML}}$  range. The range for proper hybrid mode-locking however, is restricted as can be seen (Fig. 7(b), right panel) by strong spectral components around the natural QDL resonance frequency below  $f_{\text{HML}} \sim 4.2$  GHz and above  $f_{\text{HML}} \sim 4.5$  GHz, where the laser mode-locks at its native and hybrid frequencies. The asymmetry in the frequency range for hybrid mode-locking around the native mode-locking frequency has been observed in other HMLQDLs as well [27]. The intensity variations in the modulated injection laser spectrum as a function of wavelength for a certain  $f_{\text{HML}}$  can be a sign of self phase modulation due to gain saturation in the gain section of the HMLQDL.

An optimum in spectral width of the modulated CW laser was found for  $I_{\text{injection}} \sim 750$  mA and  $f_{\text{HML}} \sim 4.45$  GHz. This point approximately coincides with  $I_{\text{injection}}$  where the passively mode-locked QDL starts to give spurious frequencies in the RF spectrum, and where  $f_{\text{HML}}$  coincides with the passive mode-locking frequency at this value of  $I_{\text{injection}}$ . The largest spectral width of the modulated CW injection laser, determined at -20 dBc, was 1.27 nm with an injected power of 6.2 mW into the 25% port. The working point for further investigation was chosen at  $I_{\text{injection}} = 747.3$  mA and  $f_{\text{HML}} = 4.4532$  GHz.

#### 4. Characterization of the generated frequency comb

In order to characterize the discrete modulation side-bands (these will be called comb modes from now on) imposed on the injected CW laser, high-resolution optical spectra were taken to resolve the individual comb modes. To conclude the measurements on the generated frequency comb the optical coherence of the comb modes has been verified in an optical heterodyne-beat experiment with two CW lasers and an  $\text{Er}^{3+}$ -fiber frequency comb laser.

##### 4.1. High resolution optical spectra of the generated frequency comb

The setup of Fig. 2 has been used to acquire high-resolution optical spectra of the generated frequency comb. The CW probe laser was in this case an Agilent 8164A with 81600B tunable laser source (relative set accuracy  $< \pm 125$  MHz, linewidth  $\sim 100$  kHz, frequency stability within tens of MHz). The optical beat with the injection laser was used to characterize the generated comb. The frequencies of these comb modes are positioned at the optical injection frequency ( $f_{\text{injection}}$ ) modulo  $f_{\text{HML}}$ . The probe laser frequency was stepped through the generated comb spectrum in steps of 1–2 GHz.

With this setup optical spectra with high frequency resolution (120–600 kHz) have been measured, and a determination of the comb amplitude to background ratio could be derived from these spectra. About 1% of the light after the SOA was sent to the OSA for low resolution reference spectra, while 99% of the light was used to generate the optical heterodyne beat between the optically injected HMLQDL and the probe laser. The resulting RF spectra were measured with the ESA.

Once  $f_{\text{injection}}$  was established (in this case relative on the Agilent 81600B wavelength scale), the comb modes can be found and the peak height and signal to background ratio determined from the RF spectra by a fitting procedure. The radio band width (RBW) of the ESA was set at  $\geq 300$  kHz in order to properly record the RF power of the down converted optical modes in

the photo diode signal.

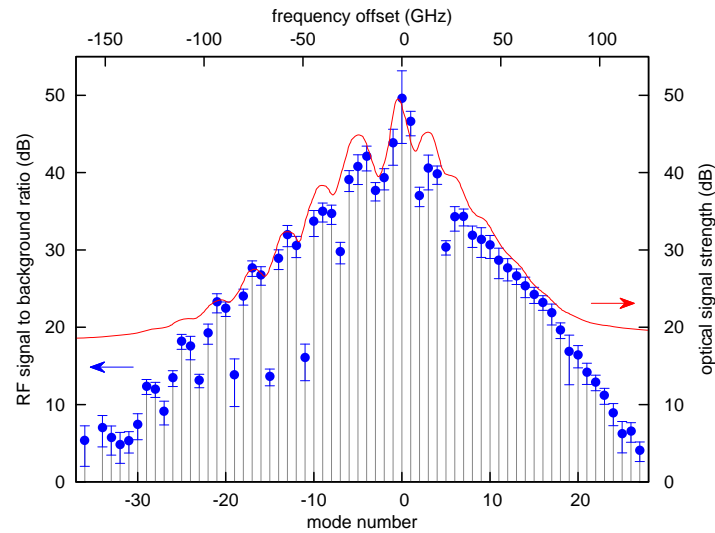


Fig. 8. The signal to background ratio of each of the modes of the comb generated by the HMLQDL on the CW injection laser. Each dot represents a mode of the comb. The error bars give the rms deviation. The average of the OSA spectra recorded during the probe laser scan is given by the red line. The gain profile of the quantum dot laser is nearly constant on the wavelength scale of this plot.

Figure 8 shows the determined signal to background ratio for each side mode of the modulated CW laser. Mode position 0 equals  $f_{\text{injection}}$ . The average of the OSA spectra recorded during the high-resolution scan is given as a comparison (red line). The OSA wavelength scale has been calibrated with the Agilent 81600B and the peak value of the OSA was shifted to match the peak value of mode 0. The width of modulated CW laser from 0 to -20 dBc as seen on the OSA spectra can directly be compared with the width of the modulation in the high-resolution optical spectrum. The 30 dB signal to background ratio spans 23 modes, which is  $> 100$  GHz in the optical domain. These data show that we have generated a frequency comb existing of narrow modulation peaks, through modulation of the injected CW laser by the HMLQDL.

The occasional mode with a low signal to background ratio is possibly a sign of self phase modulation due to saturation in the gain section of the HMLQDL structure [28]. The asymmetry in the spectrum can be seen as a hint in this direction, as well as the fact that the modulation of the spectral intensity was observed when the power of the light coupled into the laser was relatively high, while  $I_{\text{injection}}$  was, at the same time, set for optimal modulation width. Despite the long measurement time causing significant deviation in the fiber in-coupling ( $> 5$  dB) which might have led to varying laser dynamics during the measurement, the generated comb was not much affected. The recorded OSA spectra show a slight variation over time. However, the correspondence of the high-resolution spectrum with the averaged OSA spectra show that these variations were not the prime cause of the reduced signal to background of some of the modes.

In a separate heterodyne beat measurement, using two Toptica DL 100/pro lasers as probe and injection laser, we determined the width of the comb modes on short time scales by use of the ESA. In this case the RBW of the ESA was set below the linewidth of the optical heterodyne beat, in order to resolve the width of the individual modes of the comb. The width of the heterodyne beat between the injection and probe laser was determined to be 140(60) kHz. The width of the heterodyne beat between comb mode 18 of the generated comb and the probe laser

was 160(40) kHz, and the width of the heterodyne beat of comb mode 39 with the probe laser was 170(90) kHz. This means that there is no significant broadening of the generated comb modes with increasing mode number within the errors.

#### 4.2. Optical coherence of the generated frequency comb

The coherence of the generated comb was determined by an optical heterodyne experiment involving two CW lasers and an  $\text{Er}^{3+}$ -fiber frequency comb laser (FCL) as shown in Fig. 9. Two Toptica DL 100/pro CW diode lasers were used in this experiment. Beat frequencies ( $f_{\text{beat}}$ ) of both CW lasers with the FCL were counted. The optical beat frequency of the second CW laser with a mode of the generated comb on the injected CW laser was also counted. The counters (Agilent 53132A) were synchronously gated using an external trigger and time gate. The FCL, ESA, counters and RF generator used to generate  $f_{\text{HML}}$  were all referenced to a rubidium atomic standard (Stanford Research Systems PRS10) phase-locked to a one pulse-per-second signal retrieved from the global positioning system.

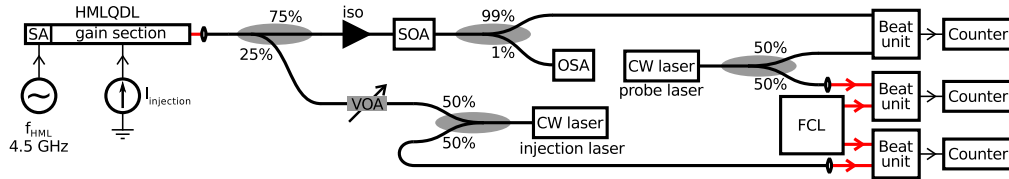


Fig. 9. Setup used to characterize the coherence of the comb generated on the CW injection laser. HMLQDL: hybridly mode-locked quantum dot laser, iso: isolator, SOA: semiconductor optical amplifier, OSA: optical spectrum analyzer, FCL: frequency comb laser, VOA: variable optical attenuator, thin black lines: electrical signals, red lines: free space optical path, thick black lines: fiber optics.

Each mode of the QDL generated comb and fiber frequency comb laser can be described by  $f_n = f_{\text{CEO}} + n f_{\text{rep}}$ ,  $n \in \mathbb{N}$ , where  $f_{\text{CEO}}$  is the carrier envelope offset frequency,  $f_{\text{rep}}$  is the repetition rate frequency of the comb, and  $n$  the mode number of the comb mode. The frequency  $f_{\text{CW}}$  of a CW laser in an optical heterodyne measurement with a FCL can be expressed as:

$$f_{\text{CW}} = f_{\text{CEO}} + n \cdot f_{\text{rep}} + f_{\text{beat}}, \quad (1)$$

where  $n$  is the mode number of the optical comb mode with which the beat is made and  $f_{\text{beat}}$  is the RF beat frequency. Both  $f_{\text{CEO}}$  and  $f_{\text{beat}}$  can be positive or negative.

For two CW lasers and two FCLs (the HMLQDL generated comb being one of them) Eq. (2) and (3) can be written with  $m, n$  the mode numbers of the modes used for the optical heterodyne beats with comb<sub>1</sub> (FCL) and  $o, p$  for beats with comb<sub>2</sub> (QDL):

$$f_{\text{CW}_2} - f_{\text{CW}_1} = (n - m) \cdot f_{\text{repFCL}} + f_{\text{beatCW}_2, \text{FCL}} - f_{\text{beatCW}_1, \text{FCL}}, \quad (2)$$

$$f_{\text{CW}_2} - f_{\text{CW}_1} = (p - o) \cdot f_{\text{repQDL}} + f_{\text{beatCW}_2, \text{QDL}} - f_{\text{beatCW}_1, \text{QDL}}. \quad (3)$$

Note that  $f_{\text{CEO}}$  drops out of Eq. (2) and (3). Taking laser CW<sub>2</sub> as the injection laser,  $f_{\text{beatCW}_2, \text{QDL}} = 0$  since it acts as the central mode of the QDL generated comb. This is illustrated in Fig. 10. Equating Eq. (2) and (3) then gives:

$$\Delta f = (n - m) \cdot f_{\text{repFCL}} - (p - o) \cdot f_{\text{repQDL}} + f_{\text{beatCW}_2, \text{FCL}} - f_{\text{beatCW}_1, \text{FCL}} + f_{\text{beatCW}_1, \text{QDL}} \equiv 0, \quad (4)$$

where  $\Delta f$  is the measured deviation from 0 which is used to give a measure of the coherence of the generated comb. Measurement errors can be present when the S/N ratio of the heterodyne

beats is too low, giving rise to false or missed counts. In the experiment the three optical beat notes were counted at various counter gate times. For this experiment the CW laser frequencies do not necessarily need to be locked, therefore the lasers were left free running.

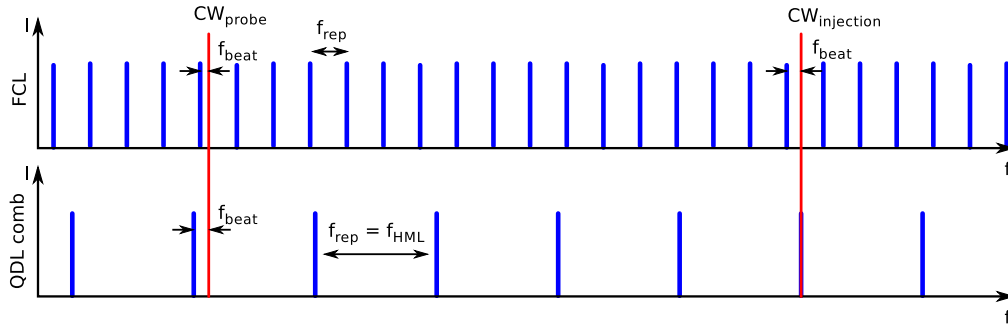


Fig. 10. Illustration of the coherence measurement by using a frequency comb laser (FCL) and the generated QDL comb. The frequency difference between the CW lasers measured with both combs should be equal ( $\Delta f = 0$ ) if the combs are coherent at the time scale of the measurement. This can be determined using the mode number differences and measured beat frequencies ( $f_{\text{beat}}$ ).

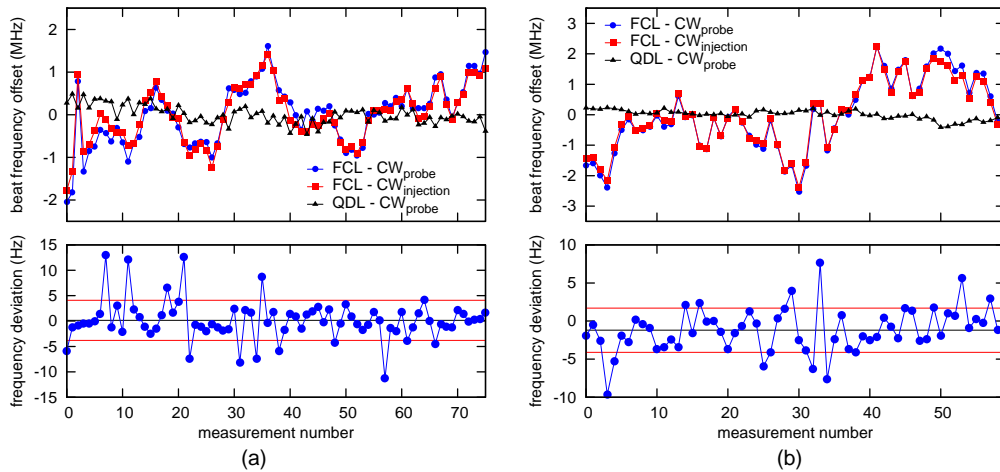


Fig. 11. Optical heterodyne beat of 2 CW lasers with the FCL and QDL comb,  $S/N > 30$  dB at  $(p - o) = 14$ , confirming the coherence of the generated comb on the CW injection laser. (a) Frequency deviation  $\Delta f = 0.1(3.9)$  Hz at 0.1 s gate time. (b) Frequency deviation  $\Delta f = -1.2(2.9)$  Hz at 2.0 s gate time. (top part) Counted beat frequencies, offset from mean in MHz. (bottom part) Frequency deviation  $\Delta f$  for  $f_{\text{beat}}$ 's from the top part in Hz.

Typical results of the measurements performed with the setup of Fig. 9 are shown in Fig. 11. The measured beat frequencies in the top part can vary with multiple MHz. The frequency deviation displayed in the bottom part of the graph was calculated from the data in the top part via Eq. (4). A measurement 14  $f_{\text{HML}}$  modes away from  $f_{\text{injection}}$ , corresponding to 249 modes frequency difference on the FCL gave deviations from Eq. (4) of -1.2(2.9) Hz at 2.0 s gate time (59 measurements), -0.1(2.6) Hz at 0.5 s gate time (61 measurements) and 0.1(3.9) Hz at 0.1 s gate time (75 measurements).

The coherence of the generated comb modes has been measured up to mode 23 of the QDL comb. In this case the S/N ratio was  $\sim 25$  dB which leads to cycle slips and/or false counts. The mean of the  $\Delta f$  measurement sets is in this case at kHz level with typical rms-deviations within the sets of up to 100 Hz.

From the measurements it is clear that the comb generated by CW injection of a HMLQDL is strongly determined by the RF generator used for hybrid mode-locking and is at least tunable in  $f_{\text{rep}}$  over the range where proper hybrid mode-locking can be achieved. The  $f_{\text{CEO}}$  of the generated comb then only relies on the absolute frequency stability of the injected CW laser. Stable optical CW laser sources at  $1.5 \mu\text{m}$  can be achieved by optical locking of the CW laser on e.g. an acetylene line [29].

## 5. Discussion of the physical processes in the modulator

The observation of coherent side mode generation from a CW laser that is injected into a HMLQDL naturally raises the question which processes could lead to the observed results. Especially in the hybridly mode-locked case it is clear that the modulation is caused by the modulation of the SA section of the QDL which acts as an electro-optical modulator (EOM). Amplitude modulation (via loss/gain) and phase modulation (via refractive index changes), can arise due to the electron-density changes in the SA section. The modulation strength might be enhanced by the quantum dot material [30]. It appears that the mode-locked laser action is not greatly influencing the side-mode generation and gives rise to the question if it is important at all for the workings of the device as an EOM.

In the case of the passively mode-locked laser, the observed small modulation depth of the injected laser can be caused by modulation of the photo-current (loss/refractive index) in the SA section of the QDL because of the light pulse circulating in the laser, and by phase modulation via the quantum dot material. In case of hybrid mode-locking this light pulse is influenced by the alternating loss and gain during the RF cycle, which causes a much stronger modulation of the CW laser. Moreover, this modulated light is then amplified in the gain section of the laser, which can give rise to non-linear optical effects if it is optically saturated. That the modulation is enhanced with gain can be seen from the increasing strength of the  $f_{\text{HML}}$  peak with increasing current in Fig. 6(b) below lasing threshold, and by the increasing width of the generated comb spectrum on the injection laser above threshold. The conclusion that gain plays a role is further supported by the fact that the width of the comb spectrum narrows when the wavelength of the injected laser is moved towards the edge of the gain spectrum of the QD material [7], where the modulation strength in the SA section and amplification in the gain section are smaller.

## 6. Conclusions and outlook

In this article, coherent modulation of a CW laser injected into a HMLQDL resulting in frequency comb generation has been demonstrated. Possible mechanisms behind this modulation have been proposed, however a full understanding is still lacking. Comb generation is possible in the gain spectrum of the QD material. The generated comb is decoupled from the HMLQDL laser action. The central frequency of the resulting comb can be changed by tuning the wavelength of the injected CW laser. Tuning of  $f_{\text{rep}}$  is provided by the hybrid mode-locking frequency of the QDL, while  $f_{\text{CEO}}$  can be tuned by using  $f_{\text{rep}}$  and the absolute frequency of the CW injection laser. The 30 dB signal to background range of the generated modulation extended over 23 modes ( $> 100$  GHz). Phase coherence of the generated comb has been shown at the level of 0.1(3.9) Hz deviation for timescales of 0.1 to 0.5 seconds, at mode 14 ( $> 60$  GHz) from the injected laser (mode 0). It provides strong evidence for full coherence of the generated comb of which more than 60 modes could be resolved.

One of the applications of these generated coherent combs could be phase locking of

telecommunication lasers on neighboring channels in dense wavelength-division multiplexing (DWDM) optical networks. Another application could be harmonic generation of a GHz RF source by optical mode filtering of the generated comb, providing stable frequency sources at  $> 100$  GHz when the light is converted back to the RF by a fast photo diode. The generated comb could also be used as a basis for several telecommunication modulation schemes. We note however, that the comb flatness (3 dB bandwidth) needs improvement, see e.g. [21, 31], before this is feasible for some of the modulation schemes proposed in the introduction.

We conclude from this experiment that coherent narrow linewidth frequency comb generation and amplification is possible in the used InAs/InP quantum dot material. Modifications to the laser cavity like a high-Q resonator and intra-cavity dispersion control, can lead to narrow linewidth ( $< 100$  kHz), short pulse ( $< 100$  fs) frequency comb lasers, paving the way towards fully integrated, robust, narrow linewidth, self referenced semiconductor frequency comb lasers.

### **Acknowledgments**

The authors thank Sylwester Latkowski for helpful comments and discussions, and W. Kaenders of TOPTICA Photonics for making available the two DL 100/pro CW diode lasers used in the present experiment. This work was supported by the Netherlands Ministry of Economic affairs through a IOP Photonic Devices program grant as well as via the MEMPHIS (Merging Electronics and Micro & Nano-Photonics in Integrated Systems) program.